

Preclinical characterization and comparison between CD3/CD19 bispecific and novel CD3/CD19/CD20 trispecific antibodies against B-cell acute lymphoblastic leukemia: targeted immunotherapy for acute lymphoblastic leukemia

Sisi Wang^{1,2,*}, Lijun Peng^{1,2,*}, Wenqian Xu^{1,2,*}, Yuebo Zhou^{1,2}, Ziyang Zhu³, Yushan Kong⁴, Stewart Leung⁴, Jin Wang (✉)^{1,2}, Xiaoqiang Yan (✉)⁴, Jian-Qing Mi (✉)^{1,2}

¹Shanghai Institute of Hematology, State Key Laboratory of Medical Genomics, National Research Center for Translational Medicine at Shanghai, Ruijin Hospital Affiliated to Shanghai Jiao Tong University School of Medicine, Shanghai 200025, China; ²Pôle Franco-Chinois de Recherche en Sciences du Vivant et Genomique, Shanghai 200025, China; ³Shanghai Blood Center, Shanghai 200051, China; ⁴Generon Biomed, Shanghai 201210, China

© Higher Education Press 2021

Abstract The CD19-targeting bispecific T-cell engager blinatumomab has shown remarkable efficacy in patients with relapsed/refractory B-cell precursor acute lymphoblastic leukemia. However, several studies showed that blinatumomab has a short plasma half-life due to its low molecular weight, and thus its clinical use is limited. Furthermore, multiple trials have shown that approximately 30% of blinatumomab-relapsed cases are characterized by CD19 negative leukemic cells. Here, we design and characterize two novel antibodies, A-319 and A-2019. Blinatumomab and A-319 are CD3/CD19 bispecific antibodies with different molecular sizes and structures, and A-2019 is a novel CD3/CD19/CD20 trispecific antibody with an additional anti-CD20 function. Our *in vitro*, *ex vivo*, and *in vivo* experiments demonstrated that A-319 and A-2019 are potent antitumor agents and capable of recruiting CD3 positive T cells, enhancing T-cell function, mediating B-cell depletion, and eventually inhibiting tumor growth in Raji xenograft models. The two molecules are complementary in terms of efficacy and specificity profile. The activity of A-319 demonstrated superior to that of A-2019, whereas A-2019 has an additional capability to target CD20 in cells missing CD19, suggesting its potential function against CD19 weak or negative CD20 positive leukemic cells.

Keywords B-cell acute lymphoblastic leukemia; bispecific antibody; trispecific antibody; CD19; CD20

Introduction

Immunotherapy has demonstrated robust clinical potency against advanced malignancies in recent years, and B cell malignancy treatment through targeted therapy has attracted considered interest [1]. The concept of bispecific T cell engager (BiTE) is to redirect T cells, irrespective of major histocompatibility complex (MHC) restriction, in close proximity to malignant cells and subsequently mediate the

cytotoxicity of T cells to tumor cells via the synapse formed between T cells and target cells [2]. Blinatumomab (Blinicyto), a scFv CD3/CD19 BiTE, was approved by the US Food and Drug Administration for the treatment of Philadelphia chromosome negative (Ph⁻) relapsed/refractory B cell precursor acute lymphoblastic leukemia (R/R pre-B ALL) in 2014 [3]. Patients with previously dismal outcomes can now achieve complete response and long-term disease remission [4]. A randomized phase III trial of patients with Ph⁻ R/R pre-B ALL showed that 44% of the patients achieved hematologic complete remission (CR) with blinatumomab, compared with 25% of the patients with standard-of-care chemotherapy [5].

Despite the clinical success, the low molecular weight of blinatumomab (~55 kDa, below the glomerular filtration threshold) leads to a short serum half-life of around 1.2 h;

Received August 19, 2020; accepted November 9, 2020
Correspondence: Jian-Qing Mi, jianqingmi@shsmu.edu.cn;
Xiaoqiang Yan, yxq3000@icloud.com;
Jin Wang, jinwang@shsmu.edu.cn

*These authors contributed equally to this work.

thus, it necessitates continuous intravenous infusion via pumps to maintain efficacy, causing substantial inconvenience in clinical practice [5,6]. To address the functional and structural limitations of blinatumomab, here we designed an anti-CD19 and -CD3 molecule, named A-319, to prolong plasma half-life [7]. We hypothesized that an improved BiTE design will exert a sufficient effect against B cell acute lymphoblastic leukemia (B-ALL) and facilitate administration in clinical settings.

Approximately 30% of blinatumomab-treated relapses are characterized by the loss of the CD19 antigen, rendering malignant cells invisible to CD19-specific immunotherapies [8–10]. One mechanism accounting for CD19 loss is the alternative exon splicing of CD19 [11]. Zah *et al.* highlighted the probability of rescuing antigen escape by spontaneous mutations and selective expansion of antigen-negative tumor cells through the targeting of additional antigens on tumor cells [12]. Therefore, one potential prophylaxis against antigen escape is to build additional antigen recognition arms into the BiTE molecule.

To potentially overcome CD19 negative relapse, we designed a trisppecific antibody, named A-2019, to target two tumor-associated antigens (TAAs; CD19 and CD20) and CD3 simultaneously. To the best of our knowledge, this is the first report of a trisppecific T cell engager designed to target two surface antigens on leukemic B cells. The CD20 antigen is one of the most widely studied B cell antigens and expressed on B cell precursor leukemic cells in up to 50% of patients [13,14]. Here, we characterized the CD3/CD19 bispecific antibody A-319 and CD3/CD19/CD20 trisppecific antibody A-2019. Superior to A-319, A-2019 recognized CD19 and CD20 because of the additional anti-CD20 single chain variable fragment (scFv) in combination with anti-CD19 scFv.

In this report, we evaluated and compared the preclinical properties of A-319 and A-2019 *in vitro*, *ex vivo*, and *in vivo*. Our results demonstrated that A-319 and A-2019 exhibited highly selective potency in the tumor cell lines *in vitro* and primary blood samples *ex vivo* with T cell activation, T cell proliferation, and cytokine production. The *in vivo* efficacy of the antibodies in inhibiting tumor growth was observed in the Raji xenograft models. The mono-targeting antibody A-319, the CD19 monovalent CD3 format, showed superior activity to A-2019, and A-2019, the CD19 and CD20 bivalent CD3 format, gained an additional function of CD20 targeting in cells missing the CD19 antigen.

Patients, materials, and methods

Patients and healthy peripheral blood mononuclear cell donors

B-ALL peripheral blood mononuclear cells (PBMCs) were

obtained with informed consent from treatment-naïve B-ALL patients ($n = 13$) in the Department of Hematology, Ruijin Hospital Affiliated to Shanghai Jiao Tong University School of Medicine, Shanghai, China. Patient PBMCs were isolated through density gradient centrifugation. Healthy donor PBMCs were collected from healthy adult volunteers in Shanghai Blood Center through density gradient centrifugation, frozen in aliquots, and stored in liquid nitrogen. Cryopreserved healthy donor PBMCs were thawed and plated 1×10^6 cells per mL in an RPMI 1640 medium (Gibco, Carlsbad, CA, USA) containing 10% fetal bovine serum (FBS, Sigma, USA).

Generation and purification of A-319 and A-2019

A-319 BiTE was generated by linking an anti-CD3 scFv to the N-terminal of an anti-CD19 fragment of antigen binding (Fab) heavy chain. Anti-CD19 and anti-CD20 scFvs were linked to the N-terminals of an anti-CD3 Fab heavy and light chains, respectively, for the generation of A-2019. The anti-CD20 scFv sequence was obtained from the anti-CD20 monoclonal antibody (mAb) rituximab. A-319 and A-2019 DNA constructs were expressed in 293 HEK cells and purified from the culture supernatants with antibody beads against the constant heavy 1 (CH1) domain of Fab.

Cell lines and *in vitro* cell cultures

B-lineage acute lymphoblastic leukemia cell line NALM6 was obtained from the Shanghai Institute of Hematology and grown in an RPMI 1640 medium (Gibco, Carlsbad, CA, USA) containing 10% fetal bovine serum (FBS, Sigma, USA) and 1% penicillin-streptomycin (Sigma, USA). The human Burkitt lymphoma cell line Raji, chronic myeloid leukemia cell line K562, and engineered cell lines K562-CD19 and K562-CD20 were obtained from Generon Biomed and grown in an RPMI 1640 medium (Gibco, Carlsbad, CA, USA) containing 10% FBS (Sigma, USA). Hygromycin B 0.4% (Sango Biotech, Shanghai, China) was then added to the K562-CD19 and K562-CD20 cell lines. The cell lines listed above were maintained at 37 °C in a humidified incubator with 95% air and 5% CO₂.

Flow cytometry

The cells were stained with the following commercial antibodies: CD4 (clone L200; BD Biosciences, USA), CD8 (clone RPA-T8; BD Biosciences, USA), CD19 (clone HIB19; BD Biosciences, USA), CD20 (clone 2H7; BD Biosciences, USA), CD45 (clone HI30; BD Biosciences, USA), CD69 (clone FN50; BD Biosciences, USA), CD25 (clone M-A251; BD Biosciences, USA), CD24 (clone ML5; BioLegend, USA), Ki-67 (clone B56; BD

Biosciences, USA), and F-actin (Phalloidin; Invitrogen, USA). Dead cells were excluded from analysis with 7-aminoactinomycin D (7-AAD) (BD Biosciences, USA). We used CytoFlex S (Beckman Coulter, USA) for *in vitro* and *ex vivo* experiments.

Multispectral fluorescence imaging

T cell and B-ALL cell synapse formations were analyzed using Amnis ImageStream Mark II. PBMCs from treatment-naïve B-ALL patients were incubated with A-319 or A-2019 for 30 min at 37 °C. Cells were stained with antibodies against CD4 (clone RPA-T4; BD Biosciences, USA), CD8 (clone RPA-T8; BD Biosciences, USA), CD24 (clone ML5; BioLegend, USA) and F-actin (Phalloidin; Invitrogen, USA). Images were captured at 40× magnification. Ideas Software version 6.2 was used for offline analysis. A gate strategy was used in identifying conjugates for the inclusion of cells with areas larger than 130 units and aspect ratios lower than 0.8. CD8 or CD4 cells were identified with a positive fluorescence gate. Immune synapse events were counted with an “erode” masking tool. In brief, individual erode masks were used on T cells (CD8 or CD4), B cells (CD24), and cytoskeleton (F-actin). Boolean logic was then applied for the creation of one unique mask identifying fluorescent pixel overlap between T and B cells. Images positive for the mask were considered synapse positive.

Quantification of CD19 and CD20 cell surface expression, *ex vivo* cytotoxicity, T cell activation, and T cell proliferation assays

The expression densities of CD19 and CD20 on the surfaces of different cell lines were determined through saturation binding with BD Quantibrite™ Beads PE fluorescence quantitation kit (BD Biosciences, USA), PE-conjugated anti-19 antibody (clone HIB19; BD Biosciences, USA), and PE-conjugated anti-CD20 antibody (clone 2H7; BD Biosciences, USA) according to the manufacturer's instructions. Maximum antibody binding values and calibration beads were used in quantifying the number of CD19 and CD20 antibody binding sites per cell. In brief, aliquots of 1×10^6 cells were stained with 100 µg/mL PE-conjugated anti-19 antibody and PE-conjugated anti-CD20 antibody, respectively. For the calculation of specific antibody binding capacity, calibration beads, which represent four populations and bear different distinct numbers of molecules, were PE-labeled, and a regression equation was generated using the quantitative calibration feature in CellQuest software. This calibration curve was used in calculating the surface molecules of CD19 and CD20 in different cell lines.

For *ex vivo* cytotoxicity analysis, specific killing was

calculated as follows: $(\% \text{ untreated CD24 positive cell viability} - \% \text{ treated CD24 positive cell viability}) / (\% \text{ untreated CD24 positive cell viability}) \times 100$. Effector T cell-to-target B cell (E:T) ratios were determined based on live cell frequencies.

The activation of CD4 and CD8 T cells was determined through CD25 and CD69 surface expression with a PE-Cy7-conjugated anti-CD25 antibody (clone M-A251; BD Biosciences, USA) and FITC-conjugated anti-CD69 antibody (clone FN50; BD Biosciences, USA) in combination with either APC-labeled anti-CD4 (clone L200; BD Biosciences, USA) or PE-labeled anti-CD8 antibody (clone RPA-T8; BD Biosciences, USA).

For the analysis of T cell proliferation, intracellular flow cytometry was conducted using a Cytotfix/Cytoperm fixation/permeabilization solution kit (BD Biosciences, USA). FITC-conjugated anti-Ki-67 antibody (clone B56; BD Biosciences, USA) was then used in assessing the level of proliferation.

Quantification of cytokines and secretion of granzyme and perforin in cell culture supernatants

After 24 and 72 h of respective culture, the supernatants were harvested and analyzed for the presence of granzyme B, perforin, TNF- α , IFN- γ , IL-6, IL-8, and IL-10 with ELISA kits (R&D Systems for granzyme B, TNF- α , IFN- γ , IL-6, IL-8, IL-10, and abcam for perforin) according to the manufacturer's instruction.

CFSE-based cytotoxicity assays

In vitro redirected T cell cytotoxicity was assayed through flow cytometry. Healthy donor PBMCs were used as effector cells, and various cell lines were used as targets. Increasing concentrations of A-319 and A-2019 were incubated with CFSE-labeled target cells and effector cells in a PBMC E:T cell ratio of 10:1. Target-cell membrane integrity was reflected by the nuclear uptake of 7-AAD. Cell lysis was determined by the decrease in CFSE positive and 7-AAD negative cells.

Human peripheral blood mononuclear cell reconstitution xenograft studies

For the *in vivo* xenograft studies, 5×10^6 /mouse fresh isolated donor human PBMCs were administered intraperitoneally at day 0. At day 3, Raji cells were harvested from the cell culture, washed twice with PBST, and resuspended in PBST. A total volume of 200 µL/mouse containing 2×10^6 Raji cells was injected subcutaneously into the left flank of NOD-SCID γ chain-deficient (NSG) mice. The mice were treated with different doses of antibodies or control vehicles when the tumor size reached

approximately 100 mm³. Mice were weighed, and tumor volume was determined with external caliper measurements and calculated using a standard hemispheroid formula. The mice were sacrificed when the tumor volume reached around 3000 mm³. Each result was presented as the arithmetic mean for each group.

Statistical analysis

Graphical and statistical analysis were performed using GraphPad Prism 8.0 (GraphPad Software Inc., San Diego, CA, USA). *Ex vivo* and *in vitro* differences between groups were analyzed using paired Student *t* test, unpaired Student *t* test, and Wilcoxon matched-pairs signed rank test. One-way and two-way ANOVA analysis were performed for comparison in terms of *in vivo* tumor growth inhibition. $P < 0.05$ indicated statistically significant data.

Results

Construction, generation and purification of A-319 and A-2019

As shown in Fig. 1A, A-319 contained an anti-CD3 scFv linked through linker to the N-terminal of the heavy chain of an anti-CD19 Fab fragment. Anti-CD19 and anti-CD20 scFvs were linked to the N-terminals of an anti-CD3 Fab heavy and light chains, respectively, for the generation of A-2019. A-319 and A-2019 were expressed and produced by 293 HEK cells and purified from the culture supernatants by using antibody beads against the CH1 domain of Fab. In SDS-PAGE, a single band of approximately 67 kDa in A-319 and another band of 85 kDa in A-2019 in respective nonreducing condition were observed (Fig. 1B), showing that the two constructs expressed homogenous proteins with expected molecular weights.

A-319 and A-2019 promote synapse formation between autologous B and T cells in B-ALL patients

To verify that A-319 and A-2019 mediate the simultaneous engagement of B cells and T cells, we used imaging flow cytometry to measure *ex vivo* B/T cells immune synapse formations in the coculture of PBMCs from seven treatment-naïve B-ALL patients and A-319, A-2019, or no antibody (CD8 T cells were not detected in one patient blood sample). After 30 min of incubation, we observed an apparent immune synapse on the interface of B/T cell induced by A-319 and A-2019. When the coculture was performed without an antibody, no synapse formation was observed (Fig. 2A). At a dose of 20 pmol/L, A-319 induced synapse formations in 0.94% (95% CI 0.03–1.85) of CD4 T cells and 0.58% (95% CI 0.04–1.12) of CD8 T cells. By contrast, only 0.39% (95% CI 0.01–0.76) of CD4

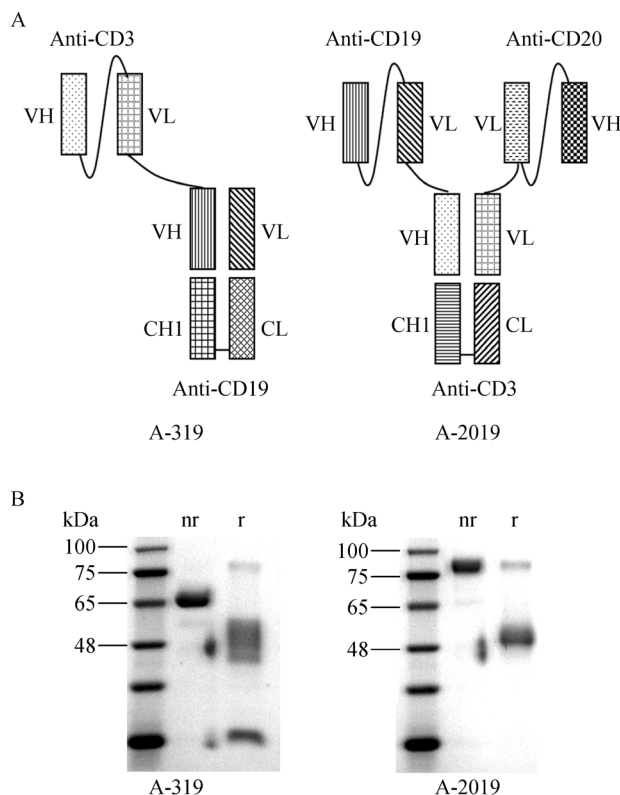


Fig. 1 Schematic and purification of A-319 and A-2019. A-319 and A-2019 were produced by using expression vector-transfected 293 HEK cells and through purification from culture supernatants with antibody beads against constant heavy 1 (CH1) domain of Fab and SDS-PAGE analysis. (A) Structures of A-319 and A-2019. A-319 is composed of anti-CD3 scFv and anti-CD19 Fab fragment, and A-2019 is composed of anti-CD3 Fab fragment, anti-CD19 scFv, and anti-CD20 scFv. (B) SDS-PAGE and Coomassie blue staining of purified A-319 (left) and A-2019 (right). Nonreducing (nr) and reducing (r) SDS-PAGE of A-319 and A-2019 are shown.

T cells and 0.14% (95% CI –0.07–0.36) of CD8 T cells were recruited by A-2019 to form synapses ($P < 0.05$; Fig. 2B).

A-319 and A-2019 elicit specific cytotoxicity in various cell lines *in vitro*

We procured and produced several cell lines (K562, K562-CD19, K562-CD20, NALM6, and Raji) with varied CD19 and CD20 expression levels. To assess the specificity and potency of A-319 and A-2019, we measured surface expression within the cell lines. CD19 ranged from 1987 to 31 430, and CD20 ranged from 1274 to 39 303 molecules per cell (Table 1). Then, we determined the efficiency and specificity of A-319 and A-2019 in inducing specific T cell cytotoxicity against target cells by performing killing assays in the cocultures of healthy PBMCs and different tumor cell lines in an E:T ratio of 10:1 for 24 h at different

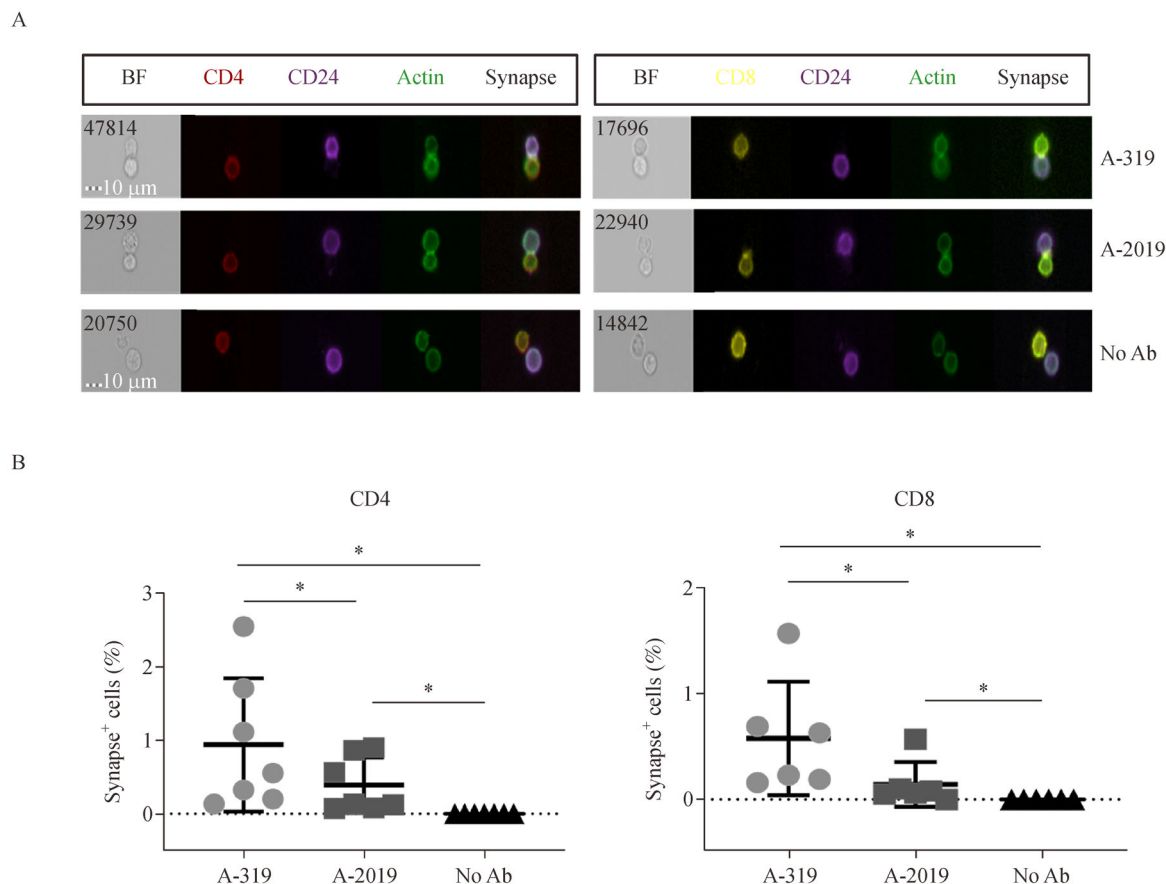


Fig. 2 Qualitative and quantitative analysis of *ex vivo* immune synapses of autologous B and T cells induced by A-319, A-2019, and no antibody. PBMCs from treatment-naïve B-ALL patients were cultured with either A-319 or A-2019 for 30 min at 37 °C. Cells were stained with labels against CD4 (red), CD8 (yellow), CD24 (purple), and F-actin (green) and B/T cell synapses were analyzed using imaging flow cytometry. (A) Representative images of B/T cell synapse (A-319, top panel and A-2019, middle panel) and non-synapse B/T cell doublets (No Ab, bottom panel) are shown. B/T cell synapses demonstrate fluorescence overlapping with CD24, F-actin, and CD4 (left) or CD8 (right) signals at 40× magnification. BF, bright-field. (B) Qualitative analysis of the immune synapse between autologous B and T cells induced by A-319 and A-2019. Percentage of CD4 or CD8 T cells involved in synapse formation with B cells are shown. Asterisks indicate statistical significance. * $P < 0.05$.

antibody doses (Fig. 3A–3E). As expected, no lysis redirected by A-319 and A-2019 was observed in the CD19/CD20 double-negative cell line K562 (Fig. 3A). A-319 and A-2019 mediated potent lysis in a dose-dependent manner in cell lines with different levels of CD19 expression (Raji, NALM6, and K562-CD19) (Fig. 3B–3D). A-319 demonstrated lysis with EC_{50} value in the lower picomolar value of 0.18, 0.32, and 0.40 in Raji, NALM6, and K562-CD19, respectively, and A-2019 EC_{50} values were high at 0.54, 1.65, and 1.22 pmol/L in the three cell lines (Table 1). Both molecules achieved maximum killing in these cell lines (Fig. 3B–3D). The specificity of A-2019 to CD20 was demonstrated by the killing of a CD20 single-positive cell line K562-CD20 at EC_{50} of 3.39 pmol/L whereas A-319 failed to show CD20 targeting (Fig. 3E, Table 1).

To investigate how A-319 and A-2019 trigger specific lysis, we analyzed the secretion of granzyme B and

perforin from the supernatants of Raji cells after stimulation of PBMC for 24 h. A-319 and A-2019 mediated granzyme B and perforin secretion of PBMCs with superior effects observed upon A-319 (Fig. 3F).

A-319 and A-2019 mediate autologous *ex vivo* B cell depletion in primary B-ALL blood samples with the induction of T cell activation, T cell proliferation, and cytokine release

Given that primary B cells in B-ALL peripheral blood samples express different patterns and levels of CD19 and CD20, we tested the ability of A-319 and A-2019 to activate and proliferate T cells, mediate the depletion of autologous B cells, and induce cytokine release. First, we determined the effects of A-319 and A-2019 on the stimulation of T cells with autologous B cells as targets. Six patients were included in different assays. Patient

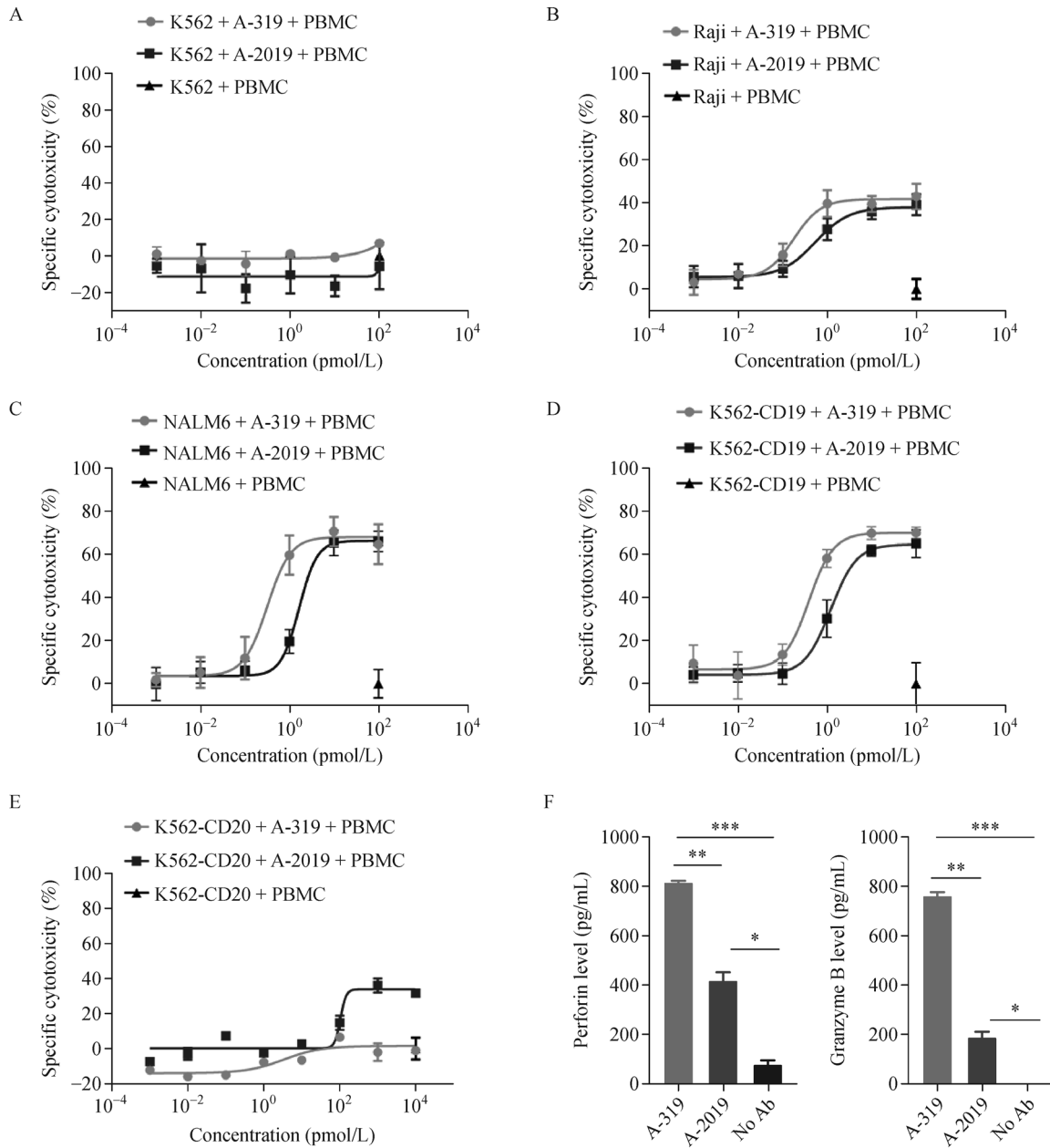


Fig. 3 A-319 and A-2019 mediated specific cytotoxicity in different cell lines *in vitro*. Redirected T cell cytotoxicity was assayed through flow cytometry using healthy donor PBMCs as effector cells and various cell lines as targets. Increasing concentrations of A-319 and A-2019 were incubated with CFSE-labeled target and effector cells in an E:T ratio of 10:1 for 24 h. (A–E) Percent of tumor target lysis in CD19⁻/CD20⁻ K562, CD19⁺/CD20⁺ Raji, CD19⁺/CD20⁻ NALM6, CD19⁺/CD20⁻ K562-CD19, and CD19⁻/CD20⁺ K562-CD20 cells were determined through flow cytometric analysis. (F) Culture supernatants were analyzed for perforin (left) and granzyme B (right) levels induced by A-319 and A-2019 after 24 h coculture of PBMC and Raji cells. Asterisks indicate statistical significance. * $P < 0.05$; ** $P < 0.005$; *** $P < 0.0005$.

Table 1 Quantification of CD19 and CD20 cell surface molecules of each cell line (K562, K562-CD19, K562-CD20, NALM6, and Raji) and the respective EC₅₀ value (pmol/L) of specific killing mediated by A-319 and A-2019

Cell line	Surface molecules per cell		EC ₅₀ (pmol/L)	
	CD19	CD20	A-319	A-2019
K562	1987	1274	/	/
K562-CD19	8413	2222	0.40	1.22
K562-CD20	2335	39 306	/	3.39
NALM6	31 430	2138	0.32	1.65
Raji	28 016	25 673	0.18	0.54

PBMCs were incubated with antibodies for 16 and 24 h, then FACS analysis was performed for the evaluation of T cell activation. The results of representative patient sample are shown in Fig. 4A (16 h) and 4B (24 h). A-319 and A-2019 induced the activation of CD4 and CD8 T cells, as evidenced by the upregulation of CD25 and CD69 expression. Notably, the expression of CD69, an early activation marker of T cells, was higher than that of CD25 in CD4 or CD8 T cells at 16 h. At 24 h, the expression of intermediate T cell activation marker CD25 increased and exceeded that of CD69 (Fig. 4A and 4B). When the activation effects were compared between A-319 and A-2019, A-2019 showed lower capacity at 20 pmol/L.

Consistent with the data of T cell activation, A-319 and A-2019 induced the proliferation of T cells after 72 h incubation; at 2.0 and 20 pmol/L, A-319 demonstrated more enhanced T cell proliferation than A-2019 (Fig. 4C). The activation and proliferation of T cells subsequently led to targeted cell lysis. A-319 and A-2019 induced potent *ex vivo* autologous B cell lysis at 72 h. A-319 and A-2019 demonstrated dose-dependent potency at 0.2, 2.0, and 20 pmol/L and achieved nearly equal killing of approximately 75% at 20 pmol/L (Fig. 4D), which was in line with the results obtained from experiments in the cell line killing assay. Furthermore, A-319 and A-2019 induced the secretion of cytokines (IL-6, IL-8, IL-10, TNF- α , and

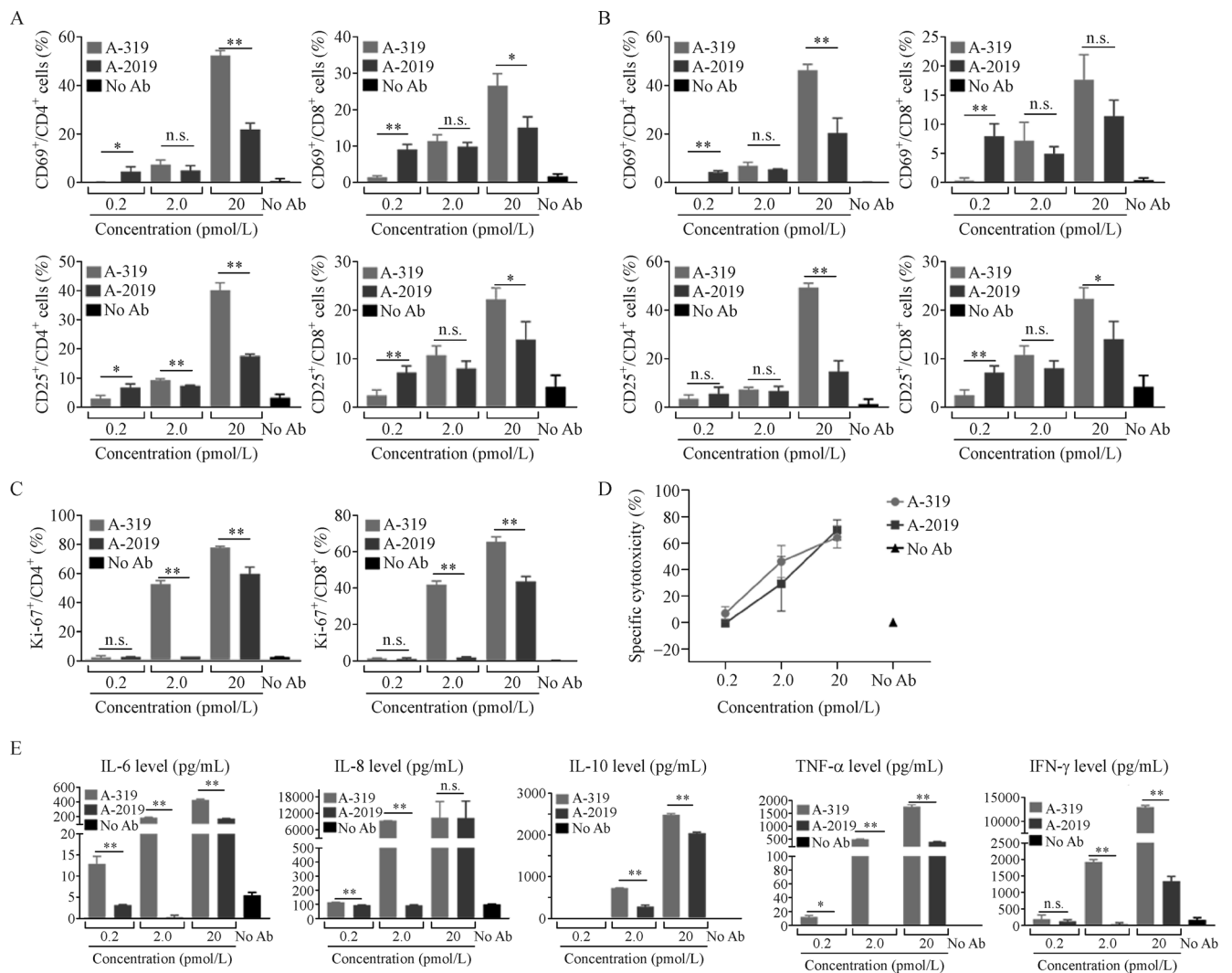


Fig. 4 A-319 and A-2019 induced potent *ex vivo* T cell activation and proliferation, B cell depletion, and cytokine release in primary B-ALL patients. PBMCs from treatment-naïve B-ALL blood samples were isolated and cocultured with an increasing dose of A-319 or A-2019 at different time periods. Flow cytometry analysis was then performed for the assessment of the efficacy of the two antibodies. (A, B) Upregulation of CD69 and CD25 on CD4 and CD8 T cell induced by A-319 and A-2019 for early activation at 16 h (A) and intermediate activation at 24 h (B). (C) T cell proliferation induced by A-319 and A-2019 was demonstrated by the upregulation of Ki-67 of CD4 and CD8 T cells in a dose-dependent manner after 3 days of incubation. (D) B cell cytotoxicity mediated by A-319 and A-2019 in a dose-dependent manner after 3 days of incubation. (E) Supernatants of cell cultures were harvested after 3 days of incubation and levels of IL-6, IL-8, IL-10, TNF- α , and IFN- γ were measured with ELISA. Asterisks indicate statistical significance. * $P < 0.05$; ** $P < 0.005$. n.s., no significance.

IFN- γ), and A-319 demonstrated dose dependence (Fig. 4E). A-2019 induced cytokine release to a lower degree and may have attenuated the level of cytokine storm. Overall, A-319 and A-2019 mediated T cell activation, T cell proliferation, B cell depletion, and cytokine release in patient PBMC samples.

In vivo tumor growth inhibition by A-319 and A-2019

The potent *in vitro* cytotoxicity of the two constructs prompted us to examine whether they can inhibit tumor growth *in vivo*. NSG mice were grafted with freshly isolated donor PBMCs through intraperitoneal injection. After 2 days, Raji cells were engrafted subcutaneously. When the tumor volume reached approximately 100 mm³, the mice were treated with A-319 (10 μ g/kg), A-319 (50 μ g/kg), A-2019 (50 μ g/kg), A-2019 (250 μ g/kg), or vehicle control PBST daily through intraperitoneal infusion for 21 days. All the animals survived until the scheduled termination.

All antibodies administered were well tolerated, as was

shown in Fig. 5A. Relative change in body weight (RCBW) fluctuated at a certain range of $\pm 10\%$, and no significant weight differences were observed among different groups. Tumor growth inhibition was then measured (Fig. 5B and 5C). Similar to the *in vitro* findings, significant antitumor activity was observed in the group that received A-319 at 50 μ g/kg with huPBMC immune reconstitution, suggesting that A-319 is capable of inhibiting tumor growth *in vivo*. However, A-2019 was inferior to A-319 in terms of tumor growth inhibition. A high dose of A-2019 (250 μ g/kg) administration failed to induce the same tumor growth inhibition (TGI) as that induced by a low dose of A-319 29 days after administration (Fig. 5B and 5C). Dose-dependent decrease in tumor volume were detected in mice with A-319 and A-2019 (Fig. 5B and 5C). Fig. 5D shows the percentages of human CD4 and CD8 in peripheral blood after the mice were sacrificed at the end of the experiment, indicating human PBMC reconstitution status of each group. The data suggested that A-319 showed more robust and potent *in vivo* antitumor activities than A-2019 in the Raji engraftment models.

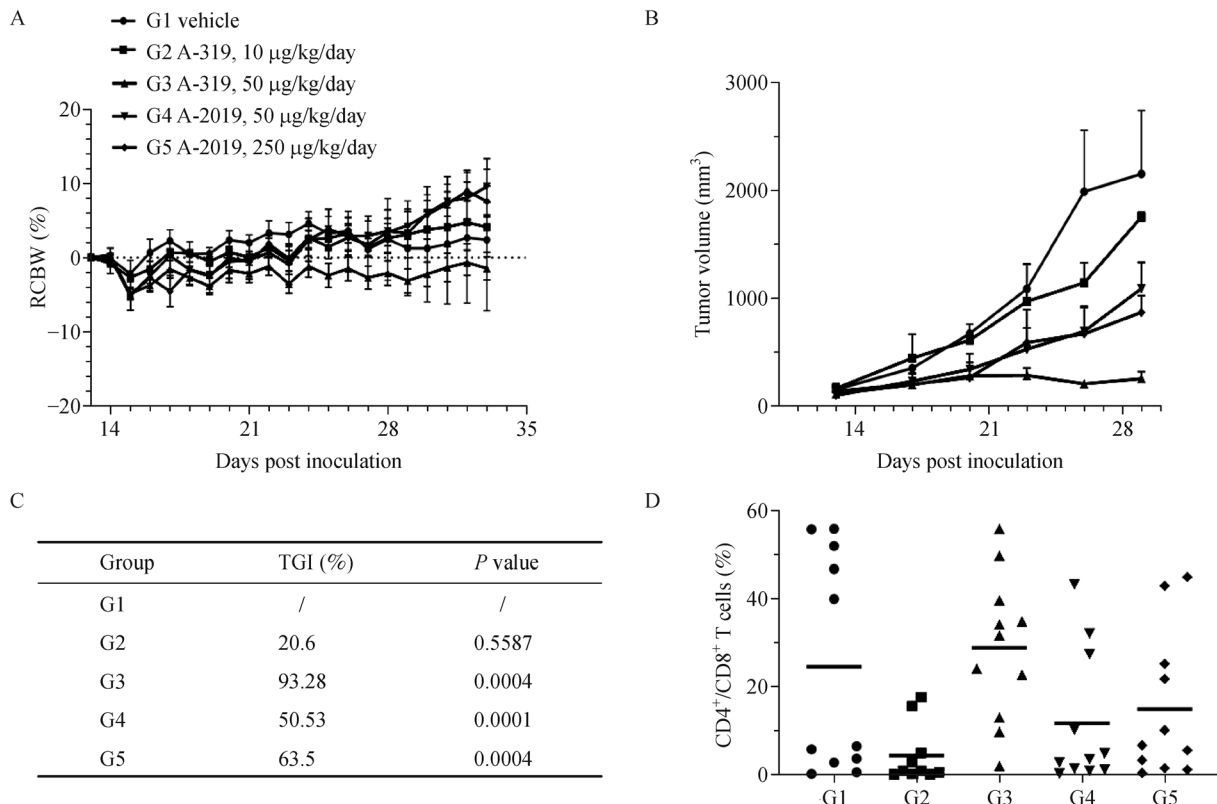


Fig. 5 *In vivo* antitumor activities of A-319 and A-2019 in the Raji xenograft models. The mice were injected with human PBMCs into the peritoneal cavity. Subcutaneous Raji tumor growth reached a volume of approximately 100 mm³ after 13 days. The mice were then allocated to the treatment groups and received daily treatment for 21 consecutive days with vehicle control PBST, A-319 (10 μ g/kg), A-319 (50 μ g/kg), A-2019 (50 μ g/kg), or A-2019 (250 μ g/kg) through intraperitoneal infusion. (A) RCBW of Raji xenografts in different treatment groups. (B) Tumor growth curve of each group. (C) TGI and *P* value of each group. (D) Percentages of human CD4 and CD8 T cells in peripheral blood lymphocytes of Raji xenografts showed the huPBMC reconstitution of each mouse.

Discussion

Blinatumomab is a potent CD19-targeted BiTE but its relative short half-life limits the function of BiTE to around 2 h; thus, continuous intravenous use is necessary to ensuring clinical efficacy [5,6]. We presented here a CD3/CD19 BiTE, A-319, with the expectation to minimize clinical inconvenience. The CD19-antigen escape with blinatumomab leaves patients with limited therapeutic options; thus, treatments for eliminating relapsed diseases are necessary. Here, we designed A-2019, a novel CD3/CD19/CD20 trisppecific antibody with dual-function to kill leukemic cells expressing either CD19 or CD20. The addition of anti-CD20 recognition arm was introduced owing to the following reasons: first, the ubiquitous expression of CD19 and CD20 on B cells makes it an extremely low-possibility event that both antigens lose simultaneously; thus, the aim was to decrease the escape of B cells in the target treatment of B-ALL [15]; second, the anti-CD20 scFv in the A-2019 construct was derived from the anti-CD20 monoclonal antibody rituximab. Rituximab is a clinically validated chimeric anti-CD20 monoclonal antibody and has become a standard care agent for non-Hodgkin's lymphomas, such as follicular lymphoma, diffuse large B cell lymphoma, chronic lymphocytic leukemia, and mantle cell lymphoma [16]. The benefits of the construct for B-ALL treatment is the improved outcomes after rituximab is used as an addition to the intensive chemotherapy of patients suffering from CD20 positive pre-B ALL and younger than age 55–60 years [17]. Therefore, A-2019 with dual-recognition to CD19 and CD20 is expected to serve as a safeguard against the escape of CD19 negative tumor cells.

We previously tested various combinations of anti-CD3 scFv/Fab, anti-CD19 scFv/Fab, and anti-CD20 scFv. The optimal constructs of the CD3/CD19 bispecific antibody (A-319) and the CD3/CD19/CD20 trisppecific antibody (A-2019) were selected according to the prominent capacity of cancer cell depletion. Our results showed the potential of A-319 and A-2019 in the treatment of B-ALL. Both molecules are capable of immune synapse induction, CD4 and CD8 T cell activation and proliferation, cytokine production, and CD19 positive B cell elimination, and A-2019 is effective for CD20 positive B cells. A-319 and A-2019 demonstrated potent *in vivo* activity in the Raji xenograft mouse models. We expect that A-319 will demonstrate more favorable pharmacokinetic property than blinatumomab. As previously described, anti-CD19 Fab fragment was used instead of the scFv domain in constructing A-319. This approach increased the molecule weight to approximately 67 kDa and serum half-life. These resulting features may benefit B-ALL patients because dosing frequency can be reduced (twice IV infusion, Table S1) while blinatumomab requires continuous infusion to maintain potent drug concentration [6].

The vulnerability of blinatumomab treatment to antigen escape has been highlighted by multiple cases of relapse resulting from the emergence of CD19 negative leukemic cells [8,9]. Sotillo *et al.* reported that one of the mechanism of CD19 loss relapse was the alternative splicing of the CD19 gene that leads to the expression of variants lacking the domains required for recognition by CD19-targeted therapies [11]. To mitigate CD19 negative relapses, a novel antibody, A-2019, capable of triggering T cell responses on the target cells expressing either CD19 or CD20, was introduced. Our results showed that A-2019 can kill CD20 single-positive cell line K562-CD20, indicating its specificity against CD20. Thus, using A-2019 may represent a novel strategy for preventing CD19 negative relapse and treating patients with CD19 negative relapse. Furthermore, in comparison to blinatumomab, A-2019 is expected to show a more favorable safety profile. For example, neurotoxicity was reported as a serious side effect of blinatumomab [18–20]. In a phase 2 study of adult R/R pre-B ALL patients treated with blinatumomab, 52% patients had neurologic events, including tremor, dizziness, and confusion state [21]. Mural cells, surrounding the endothelium and critical for blood-brain-barrier integrity, were found to express CD19, suggesting an on-target mechanism for neurotoxicity in CD19-directed therapies [22]. A-2019 binds to CD19, which has a lower affinity than blinatumomab (1.06×10^{-8} mol/L vs. 1.49×10^{-9} mol/L, respectively; Table S1). Thus, the risk of concomitant neurotoxicity is low [23].

Although A-319 and A-2019 are effective in killing CD19 and CD20 double positive cells, they show different levels of potency. A-319 is superior to A-2019 in terms of efficacy. As shown in Table S1, A-319 and blinatumomab demonstrated comparable EC_{50} values in human B cells and B cell line Raji. This result indicated that A-2019 is inferior to blinatumomab in terms of potency. Our data indicated that the level of potency of the dual-recognition molecule does not exceed that of a mono-recognition antibody, in contrast to a previous result [24]. The results can be exemplified by the difference in T cell recruitment capability of A-319 and A-2019. A-319 induced more immune synapse formations than A-2019 in the CD4 and CD8 T cells, indicating A-319 is more efficient in recruiting T cells. Enhanced T cell activation followed by T cell recruitment results in increased T cell proliferation and targeted lysis of A-319. The difference in efficacy may be attributed to a number of factors, including the binding epitopes of the antibodies, structures of A-319 and A-2019 molecules, and expression levels of the CD19 and CD20 on target cells. Notably, despite that the molecules are comparable in terms of *in vitro* killing capacity in PBMCs, a general decrease in overall cytokine induced by A-2019 was observed. In particular, in terms of secretion of IL-6 and IFN- γ , which are two key cytokines leading to cytokine release syndrome (CRS), A-2019 induced

significantly lower secretion level than A-319. As seen in Table S1 that A-319 and blinatumomab demonstrated similar cytokine induction, A-2019 is expected to lower the risk of CRS, suggesting that A-2019 trades efficacy with a safer profile, and this trade-off may be applied to the case of CD19-negative relapse as relapsed patients are normally in a poor condition.

In summary, the preclinical data presented in this manuscript demonstrated that A-319 is a potent bispecific antibody. With increased molecular size, it would benefit patients with B-ALL because of reduced dosing frequency. As for A-2019, the two recognition arms to CD19 and CD20 pave the way to function against CD19 negative relapsed patients.

Acknowledgements

This study was funded by the National Natural Science Foundation of China (Nos. 81670147, 81570178, and Antrag M-0377), Shanghai Municipal Education Commission-Major Project for Scientific Research and Innovation Plan of Natural Science (No. 2021-01-07-00-02-E00091), and Gaofeng Clinical Medicine Grant Support of Shanghai Municipal Education (No. 20172002).

Compliance with ethics guidelines

Xiaoqiang Yan, Stewart Leung, and Yushan Kong are employees of Generon Biomed Shanghai dedicated to the development of bispecific antibodies for immunotherapy. Sisi Wang, Lijun Peng, Wenqian Xu, Yuebo Zhou, Ziyang Zhu, Jin Wang, and Jian-Qing Mi declare no competing financial interests. All procedures performed in studies involving human blood samples were approved by the ethics committee at Ruijin Hospital Affiliated to Shanghai Jiao Tong University School of Medicine and Shanghai Blood Center and performed according to the principles of the 1964 *Declaration of Helsinki* and its later amendments or comparable ethical standards. All institutional and national guidelines for the care and use of laboratory animals were followed. All patients and healthy blood donors gave written informed consent prior to blood sample collection for the use of biomaterials and clinical data for scientific purposes.

Electronic Supplementary Material Supplementary material is available in the online version of this article at <https://doi.org/10.1007/s11684-021-0835-8> and is accessible for authorized users.

References

- Grillo-López AJ, White CA, Dallaire BK, Varns CL, Shen CD, Wei A, Leonard JE, McClure A, Weaver R, Cairelli S, Rosenberg J. Rituximab: the first monoclonal antibody approved for the treatment of lymphoma. *Curr Pharm Biotechnol* 2000; 1(1): 1–9
- Hipp S, Tai YT, Blanset D, Deegen P, Wahl J, Thomas O, Rattel B, Adam PJ, Anderson KC, Friedrich M. A novel BCMA/CD3 bispecific T-cell engager for the treatment of multiple myeloma induces selective lysis *in vitro* and *in vivo*. *Leukemia* 2017; 31(8): 1743–1751
- Guerra VA, Jabbour EJ, Ravandi F, Kantarjian H, Short NJ. Novel monoclonal antibody-based treatment strategies in adults with acute lymphoblastic leukemia. *Ther Adv Hematol* 2019; 10: 2040620719849496
- Ruella M, Gill S. How to train your T cell: genetically engineered chimeric antigen receptor T cells versus bispecific T-cell engagers to target CD19 in B acute lymphoblastic leukemia. *Expert Opin Biol Ther* 2015; 15(6): 761–766
- Kantarjian H, Stein A, Gökbuget N, Fielding AK, Schuh AC, Ribera JM, Wei A, Dombret H, Foà R, Bassan R, Arslan Ö, Sanz MA, Bergeron J, Demirkan F, Lech-Maranda E, Rambaldi A, Thomas X, Horst HA, Brüggemann M, Klapper W, Wood BL, Fleishman A, Nagorsen D, Holland C, Zimmerman Z, Topp MS. Blinatumomab versus chemotherapy for advanced acute lymphoblastic leukemia. *N Engl J Med* 2017; 376(9): 836–847
- Klinger M, Brandl C, Zugmaier G, Hijazi Y, Bargou RC, Topp MS, Gökbuget N, Neumann S, Goebeler M, Viardot A, Stelljes M, Brüggemann M, Hoelzer D, Degenhard E, Nagorsen D, Baeuerle PA, Wolf A, Kufer P. Immunopharmacologic response of patients with B-lineage acute lymphoblastic leukemia to continuous infusion of T cell-engaging CD19/CD3-bispecific BiTE antibody blinatumomab. *Blood* 2012; 119(26): 6226–6233
- Cui Y, Huang Z, Zhang X, Shen W, Chen H, Wen Z, Qi B, Luo L, Tan Y, Wu Y, Kung A, Yan X. CD3-activating bi-specific antibody targeting CD19 on B cells in mono- and bi-valent format. *Blood* 2018; 132(Supplement 1): 4169
- Ruella M, Barrett DM, Kenderian SS, Shestova O, Hofmann TJ, Perazzelli J, Klichinsky M, Aikawa V, Nazimuddin F, Kozlowski M, Scholler J, Lacey SF, Melenhorst JJ, Morrisette JJ, Christian DA, Hunter CA, Kalos M, Porter DL, June CH, Grupp SA, Gill S. Dual CD19 and CD123 targeting prevents antigen-loss relapses after CD19-directed immunotherapies. *J Clin Invest* 2016; 126(10): 3814–3826
- Topp MS, Gökbuget N, Zugmaier G, Klappers P, Stelljes M, Neumann S, Viardot A, Marks R, Diedrich H, Faul C, Reichle A, Horst HA, Brüggemann M, Wessiepe D, Holland C, Alekar S, Mergen N, Einsele H, Hoelzer D, Bargou RC. Phase II trial of the anti-CD19 bispecific T cell-engager blinatumomab shows hematologic and molecular remissions in patients with relapsed or refractory B-precursor acute lymphoblastic leukemia. *J Clin Oncol* 2014; 32(36): 4134–4140
- Topp MS, Gökbuget N, Zugmaier G, Degenhard E, Goebeler ME, Klinger M, Neumann SA, Horst HA, Raff T, Viardot A, Stelljes M, Schaich M, Köhne-Volland R, Brüggemann M, Ottmann OG, Burmeister T, Baeuerle PA, Nagorsen D, Schmidt M, Einsele H, Riethmüller G, Kneba M, Hoelzer D, Kufer P, Bargou RC. Long-term follow-up of hematologic relapse-free survival in a phase 2 study of blinatumomab in patients with MRD in B-lineage ALL. *Blood* 2012; 120(26): 5185–5187
- Sotillo E, Barrett DM, Black KL, Bagashev A, Oldridge D, Wu G, Sussman R, Lanauze C, Ruella M, Gazzara MR, Martinez NM, Harrington CT, Chung EY, Perazzelli J, Hofmann TJ, Maude SL, Raman P, Barrera A, Gill S, Lacey SF, Melenhorst JJ, Allman D, Jacoby E, Fry T, Mackall C, Barash Y, Lynch KW, Maris JM, Grupp SA, Thomas-Tikhonenko A. Convergence of acquired mutations

- and alternative splicing of CD19 enables resistance to CART-19 immunotherapy. *Cancer Discov* 2015; 5(12): 1282–1295
12. Zah E, Lin MY, Silva-Benedict A, Jensen MC, Chen YY. T Cells expressing CD19/CD20 bispecific chimeric antigen receptors prevent antigen escape by malignant B cells. *Cancer Immunol Res* 2016; 4(6): 498–508
 13. Thomas DA, O'Brien S, Jorgensen JL, Cortes J, Faderl S, Garcia-Manero G, Verstovsek S, Koller C, Pierce S, Huh Y, Wierda W, Keating MJ, Kantarjian HM. Prognostic significance of CD20 expression in adults with *de novo* precursor B-lineage acute lymphoblastic leukemia. *Blood* 2009; 113(25): 6330–6337
 14. Raponi S, De Propriis MS, Intoppa S, Milani ML, Vitale A, Elia L, Perbellini O, Pizzolo G, Foà R, Guarini A. Flow cytometric study of potential target antigens (CD19, CD20, CD22, CD33) for antibody-based immunotherapy in acute lymphoblastic leukemia: analysis of 552 cases. *Leuk Lymphoma* 2011; 52(6): 1098–1107
 15. Banchereau J, Rousset F. Human B lymphocytes: phenotype, proliferation, and differentiation. *Adv Immunol* 1992; 52: 125–262
 16. Salles G, Barrett M, Foà R, Maurer J, O'Brien S, Valente N, Wenger M, Maloney DG. Rituximab in B-cell hematologic malignancies: a review of 20 years of clinical experience. *Adv Ther* 2017; 34(10): 2232–2273
 17. Thomas DA, O'Brien S, Faderl S, Garcia-Manero G, Ferrajoli A, Wierda W, Ravandi F, Verstovsek S, Jorgensen JL, Bueso-Ramos C, Andreeff M, Pierce S, Garris R, Keating MJ, Cortes J, Kantarjian HM. Chemoimmunotherapy with a modified hyper-CVAD and rituximab regimen improves outcome in *de novo* Philadelphia chromosome-negative precursor B-lineage acute lymphoblastic leukemia. *J Clin Oncol* 2010; 28(24): 3880–3889
 18. Teachey DT, Rheingold SR, Maude SL, Zugmaier G, Barrett DM, Seif AE, Nichols KE, Suppa EK, Kalos M, Berg RA, Fitzgerald JC, Aplenc R, Gore L, Grupp SA. Cytokine release syndrome after blinatumomab treatment related to abnormal macrophage activation and ameliorated with cytokine-directed therapy. *Blood* 2013; 121(26): 5154–5157
 19. Moore PA, Zhang W, Rainey GJ, Burke S, Li H, Huang L, Gorlatov S, Veri MC, Aggarwal S, Yang Y, Shah K, Jin L, Zhang S, He L, Zhang T, Ciccarone V, Koenig S, Bonvini E, Johnson S. Application of dual affinity retargeting molecules to achieve optimal redirected T-cell killing of B-cell lymphoma. *Blood* 2011; 117(17): 4542–4551
 20. Stanglmaier M, Faltin M, Ruf P, Bodenhausen A, Schröder P, Lindhofer H. Bi20 (fBTA05), a novel trifunctional bispecific antibody (anti-CD20 × anti-CD3), mediates efficient killing of B-cell lymphoma cells even with very low CD20 expression levels. *Int J Cancer* 2008; 123(5): 1181–1189
 21. Topp MS, Gökbuget N, Stein AS, Zugmaier G, O'Brien S, Bargou RC, Dombret H, Fielding AK, Heffner L, Larson RA, Neumann S, Foà R, Litzow M, Ribera JM, Rambaldi A, Schiller G, Brüggemann M, Horst HA, Holland C, Jia C, Maniar T, Huber B, Nagorsen D, Forman SJ, Kantarjian HM. Safety and activity of blinatumomab for adult patients with relapsed or refractory B-precursor acute lymphoblastic leukaemia: a multicentre, single-arm, phase 2 study. *Lancet Oncol* 2015; 16(1): 57–66
 22. Parker KR, Migliorini D, Perkey E, Yost KE, Bhaduri A, Bagga P, Haris M, Wilson NE, Liu F, Gabunia K, Scholler J, Montine TJ, Bhoj VG, Reddy R, Mohan S, Maillard I, Kriegstein AR, June CH, Chang HY, Posey AD Jr, Satpathy AT. Single-cell analyses identify brain mural cells expressing CD19 as potential off-tumor targets for CAR-T immunotherapies. *Cell* 2020; 183(1): 126–142.e17
 23. Kaplan JB, Grischenko M, Giles FJ. Blinatumomab for the treatment of acute lymphoblastic leukemia. *Invest New Drugs* 2015; 33(6): 1271–1279
 24. Gleason MK, Verneris MR, Todhunter DA, Zhang B, McCullar V, Zhou SX, Panoskaltis-Mortari A, Weiner LM, Vallera DA, Miller JS. Bispecific and trispecific killer cell engagers directly activate human NK cells through CD16 signaling and induce cytotoxicity and cytokine production. *Mol Cancer Ther* 2012; 11(12): 2674–2684